

2-aminoethyl Dihydrogen Phosphate as a Modulator of Proliferative and Apoptotic Effects in Breast Cancer Cell Lines

Manuela Garcia Laveli da Silva^{1,2}, Laertty Garcia de Sousa Cabral^{1,2}, Monique Gonçalves Alves^{1,2}, Thais de Oliveira Conceição^{1,2}, Henrique Hesse^{1,2}, Rosa Andrea Nogueira Laiso¹, Daniel da Conceição Rabelo¹ and Durvanei Augusto Maria^{1,2}

1. Development and Innovation Laboratory, Butantan Institute, Sao Paulo, SP 05503-900, Brazil

2. Faculty of Medicine, University of São Paulo, Sao Paulo, SP 01246-000, Brazil

Abstract: Background: Breast cancer is a type of cancer that affects more women throughout the world, in developing and developed countries. 2-AEH₂P is a phospholipid analog of cellular membrane, which makes it different from existing molecules for their absorption, stability and display anti-inflammatory, anti-proliferative and pro-apoptotic properties. **Methods:** MCF-7 human breast adenocarcinoma cells were treated with 2-AEH₂P. The viability and adhesion cells were evaluated by MTT assay. Cell cycle phases, apoptosis, markers and mitochondrial potential were assessed by flow cytometry. Morphological ultrastructural analyzes were performed by laser confocal microscopy. **Results:** MCF-7 Tumor cells acquired round shapes, lost cytoplasmic expansions, formed clusters in suspension and decreased significantly viability. There were changes in the morphology, membrane fragmentation and loss of cytoplasmic projection. The obtained concentrations for IC_{50%} were 37.2; 25.8; 1.8 mM for periods of 24, 48 and 72 h, respectively. Changes in the distribution of cell population phases of the cell cycle showed an increase in fragmented DNA and an increase in the G2/M phase. The expression β-gal showed proliferative reduction induced by 2-AEH₂P. Laser confocal microscopy showed changes in the mitochondrial membrane and alteration in distribution. Proliferative index of MCF-7 tumor cells treated with 2-AEH₂P decreased significantly when compared to fibroblast normal cells. The compound 2-AEH₂P is a phospholipid with antiproliferative potential and apoptosis modulator.

Key words: Human Breast Adenocarcinoma MCF-7, 2-AEH₂P, Antitumor, Apoptosis, Cell cycle, Senescence.

1. Background

Currently, breast cancer is the second most deadly cancer for women worldwide, accounting for 25.2% of all new cancer cases and approximately, 1 in 39 women will die from breast cancer [1, 2]. Conventional treatments for the condition include radiotherapy, chemotherapy and hormone therapy [3]. Statistics of probability survival and recurrence of the disease is a sign of complexity involved in the understanding of tumor pathogenesis and potential therapeutics. It is known that carcinogenesis is a multiple step process and cancer has several hallmarks:

selective proliferative advantage, altered stress response, vascularization, invasion and metastasis, metabolic rewiring, immune modulation and an abetting microenvironment [4].

The American Joint Committee on Cancer (AJCC) anatomic stage is based on extent of the cancer (in the breast, regional lymph nodes, and distant spread), while prognostic stage also includes information on the presence of estrogen receptors (ER), progesterone receptors (PR), levels of human epidermal growth factor receptor 2 (HER2, a growth-promoting protein) and/or extra copies of the HER2 gene (HER2+/HER2-), and grade (reflecting how closely the cancer's microscopic appearance looks like normal breast tissue) [5].

Corresponding author: Durvanei Augusto Maria, Ph.D., research field: pharmacology. E-mail: durvanei@usp.br.

Changes in lipid metabolism have been reported in many types of cancer. Altered metabolism is a feature that involves the development and progression of untreated breast tumors as well as resistant breast cancer. There are several regulators of breast cancer metabolism such as phosphatidylinositol-4,5-bisphosphate 3-kinase (PI3K), MYC, ER, breast cancer susceptibility gene 1 (BRCA1), and p53 [6].

The lipogenic regulatory pathways that are deregulated are mainly associated with the PI3K, Akt and mTOR pathways. In breast cancer, it includes the PI3K function gain mutation, PI3K PTEN negative regulator function loss mutation and the HER2/neu receptor tyrosine kinase (RTK) amplification and hyperactivation, which shares several downstream effectors with insulin receptor (INSR) [7-10].

The alkyl-lysophospholipid analogs (ALPs) represent a novel class of lipids with antitumor activity. The 2-aminoethyl dihydrogen phosphate (2-AEH₂P) is a primary amine is present at high intracellular concentrations in various tissues and has been implicated in several important cellular functions, such as osmoregulation, membrane stabilization, cellular division, control proliferation and neuromodulation [11]. The phospholipids such as alkylphospholipids it has been shown that favorable in treatment for cancers. These lipids are able to reduce the synthesis of phosphatidylcholine in cancer cells, influencing the turnover of phospholipids induced apoptosis [12].

The phospholipids (PLs) are interesting molecules from a biological point of view. PLs are mostly formed by a trisubstituted glycerol molecule, two fatty acids and a phosphate group. The two fatty acids substituents or apolar tail of the PLs are highly hydrophobic while the phosphate group or head is polar, therefore hydrophilic. The phosphate head is an easy reactional center, which can react with low molecular weight structures (e.g., serine, ethanolamine, glycerol, choline.) [13].

The monophosphoester 2-AEH₂P is a phosphoric ester known as aminoethyl ester phosphoric that

previously was synthesized by our group pathways. Recent studies show an antitumor effect on murine melanoma B16F10 cells, human breast adenocarcinoma MCF-7, human leukemic cells, without causing any apparent effect on normal cells [14-20].

2. Methods

2.1 Compound Preparation Monophosphoester 2-AEH₂P

The monophosphoester 2-aminoethyl dihydrogen phosphate (2-AEH₂P) was obtained from (PhosphoPure®), the pure product was analyzed in plasma by inductive coupling and mass spectrometry.

2.2 Cell Culture

The human breast adenocarcinoma MCF-7 cell line was acquired from American Type Culture Collection (ATCC® HTB-22™) and normal human fibroblast (FN1) and maintained in RPMI-1640 medium, supplemented with 10% fetal bovine serum, 100 units/mL penicillin and 100 mg/mL streptomycin. Cell was cultured in at 37 °C in a humidified atmosphere with 5% CO₂.

2.3 Colorimetric Assay

Viability of MCF-7 tumor cells was evaluated using the MTT [3-(4,5-dimethyl-thiazol-2-yl) 2,5-diphenyl tetrazolium bromide] (Sigma Chemical Co., St. Louis, MO, USA) colorimetric assay, that is based on the reduction of formazan crystals by living cells (Mosmann 1983). Briefly, MCF-7 tumor cells were seeded in 96-well tissue culture plates at 10⁴ cells per well and incubated for 24 h. The cells were treated with different concentrations of 2-AEH₂P (10 to 100 mM); control cells were treated with PBS. Then, plates were incubated at 37 °C under 5% CO₂ for 24 h. After treatment, the supernatants were removed, 100 µL of 5 mg/mL MTT solution was added to each well, and the plate was incubated for 3 h. The precipitated formazan crystals were diluted in DMSO (Sigma Chemical Co., St. Louis, MO, USA) and measured at

540 nm using the microplate reader Thermo Plate (Rayto Life and Analytical Science C. Ltd, Germany).

2.4 Cell Cycle Phases Analysis

MCF-7 tumor cells at a density of 10^6 per well were treated with 2-AEH₂P for 24 and 48 h. Cultured cells were then collected and fixed with cold 70% ethanol/20 mg/mL RNase (Sigma) and stored at -20 °C overnight. Cells were incubated at 37 °C for 45 min in 0.5 mL PBS and then stained with 1 mg/mL propidium iodide (PI) and 100 mg/mL Rnase for 30 min at 37 °C. Quantification of DNA content (10,000 events) was performed for each sample by flow cytometry. Data were acquired using the CellQuest software (Becton Dickinson) and analyzed using the ModFIT software identifying the G0/G1, S and G2/M phases of the cell cycle.

2.5 Confocal Laser Scanning Microscopy

2.5.1 Rhodamine 123

MCF-7 tumor cells were plated in 6-well and treated with 5 at 90 mM 2-AEH₂P for 24 h, then rinsed in PBS three times and stained with 10 uL rhodamine 123 (Sigma) in the dark at 37 °C; excess probe was then washed off and cells were submerged in PBS. Image analysis was performed with a confocal laser scanning microscope (Carl Zeiss LSM 700; Leica, Mannheim, Germany).

2.5.2 Acridine-Orange

MCF-7 tumor cells were plated in 6-well and treated with 5 at 90 mM 2-AEH₂P for 24 h, then rinsed in PBS three times and stained with 10 uL acridine orange – Sigma Aldrich (5 µg/mL) in the dark at 37 °C, excess probe was then washed off and live cells were submerged in PBS. Image analysis was performed with a confocal laser scanning microscope (Carl Zeiss LSM 700; Leica, Mannheim, Germany).

2.6 Measurement of Mitochondrial Membrane Potential

The mitochondrial membrane potential was

measured by rhodamine 123 prime monitored by flow cytometry. MCF-7 tumor cells at density of 10^5 cells were plated in 6-well plates and incubated for 24 h. After the cells were treated with 20, 30 and 40 mM 2-AEH₂P for 24 h. Rhodamine 123 was added at 100 mg/L 30 min before end of treatment. After washing with PBS, the cells were analyzed using a FACS can flow cytometry system (Scalibur-Becton Dickinson, San Jose, CA). A total of 10,000 cells/sample were analyzed and the mean fluorescence intensity (FL1-H channel) and percentage of cells in histogram distributes of the each population was recorded.

2.7 Cellular Senescence by β -galactosidase Activity

MCF-7 tumor cells were plated in a 96-well plate for 24 h and then treated with 10 at 50 mM 2-AEH₂P. The cells were fixed with 2% formaldehyde, 0.2% glutaraldehyde in PBS at room temperature for 5 min. After washing in PBS, cells were incubated with a solution containing 1 mg/mL β -galactosidase (Cell Signaling Technology, Danvers, MA - Kit #9860) for 16 h at 37 °C. After fixation, the cells were placed in 70% glycerol solution. Cell count was performed under a light microscope in three randomly selected fields (approximately 200 cells/field) (1 mm²) and captured for detection of senescence rate expressed in (%).

2.8 Apoptosis and Necrosis Analyzes (anexin V/PI) by Flow Cytometry

After confluence in the 6 wells plate the cells were treated with 20, 30 and 40 mM 2-AEH₂P for 24 h and then washed with PBS and resuspended in 100 uL PBS. MCF-7 tumor cells were incubated for 30 min with 1 ug of Annexin V-FITC diluted in binding buffer and 18 ug/ml propidium iodide solution. The reading of the amount of Annexin V expression (apoptosis) and PI (necrosis) will be held in flow cytometer, FACSCalibur (BD) in fluorescence intensity FL1-H/FL2-H. The results will be analyzed using WinMDI 2.8 Software.

2.9 Evaluation of Markers by Flow Cytometry

MCF-7 tumor cells treated with 2-AEH₂P and control groups were incubated for 1 h at 4 °C with 1 µg of specific antibody. Markers involved in cell death and regulators of cell cycle progression were used (Caspase 3-8 active, Bax, Bad, Bcl-2, p53, TNF-R1, PCNA, Cytochrome C, Cyclin D1). After this period the cells were centrifuged at 1500 rpm and washed with ice cold PBS and 0.2% BSA for 2 times. The supernatant was discarded and the “pellet” resuspended in 200 of Fac’s buffer containing 0.1% paraformaldehyde. The reading and analysis of the expression of receptors on the cell surface of tumor cells was performed in a FACSCalibur flow cytometer (BD) in FL-1 and the fluorescence intensity histograms acquired and analyzed using Cell-Quest-BD.

2.10 Proliferation Assay CFSE-DA

MCF-7 tumor cells treated with 2-AEH₂P and control groups were incubated with the marker carboxyfluorescein (CFSE-DA, Thermo Fisher, K1734571). CFSE-DA was diluted in PBS 0.1% human albumin at different concentrations was added to the medium and the cells with the groups treated with 2-AEH₂P and controls. The marking time was 10 min at 37 °C, homogenizing every 3 min. During dialing RPMI medium was added and incubated for 5 min on ice in the dark. Cells were washed and resuspended in 1 mL RPMI for counting. The FlowJo program provided the indices used to evaluate the spontaneous proliferation of cells labeled with CFSE, and percentage of divided cells and cell division rate indices used in this study.

3. Results

3.1 Evaluation of Cell Viability

MCF-7 tumor cells were incubated and treated with the 2-AEH₂P at concentrations of 10 to 100 mM, during 24, 48 and 72 h. After the 24 h treatment, the

MCF-7 cells lysis were morphologically observed and the cell debris formation in the supernatant from the concentration of 20 mM. The necessary concentration of 2-AEH₂P to obtain IC_{50%} was of 37.2 mM. After treated for 48 h was observed a decrease in the cell density and cell debris formation in the supernatant from the concentration of 10 mM. The IC_{50%} for the 48 h treatment was 25.8 mM of 2-AEH₂P, for 72 h was observed an intense decrease in the cell density, due the cells lysis and debris. The IC_{50%} for the 72 h treatment was 1.8 mM of 2-AEH₂P (Figure 1 A-B, Table 1).

In addition, cytotoxic effects were observed with the percentage increase of cell death, loss of cell adhesion, fragmentation of the cytoplasmic membrane and loss of progression of cytoplasmic processes (Figure 1A).

As a control group and specificity of drug action, the experiment was conducted in normal human fibroblast cells (FN1). After 24 h adhesion the FN1 cells were incubated with the 2-AEH₂P at concentrations of 10 to 100 mM at 24, 48 and 72 h. Treatment with 24 h in normal cells FN1 were observed morphological cellular lysis and little debris formation only from the concentration of 70 mM to obtain IC_{50%} in the amount of 81.8 mM. After treatment with the 2-AEH₂P 48 h, it observed little morphological appearance of cell lysis and debris formation from the concentration of 40 mM 2-AEH₂P, with IC_{50%} value of 61.6 mM. After 72 h treatment, some cells were observed with cellular lysis at concentrations of 40 mM, obtaining IC_{50%} of 44.1 mM (Figure 1 A-B, Table 1).

3.2 Analysis of the Cell Cycle Phases by Flow Cytometry

2-AEH₂P was tested to evaluate their ability to modify the distribution profile of the cell populations in the cell cycle phases. MCF-7 tumor cells were treated with the 2-AEH₂P at concentrations 30 to 70 mM for 24 h and the concentrations 20 to 50 mM after 48 h.

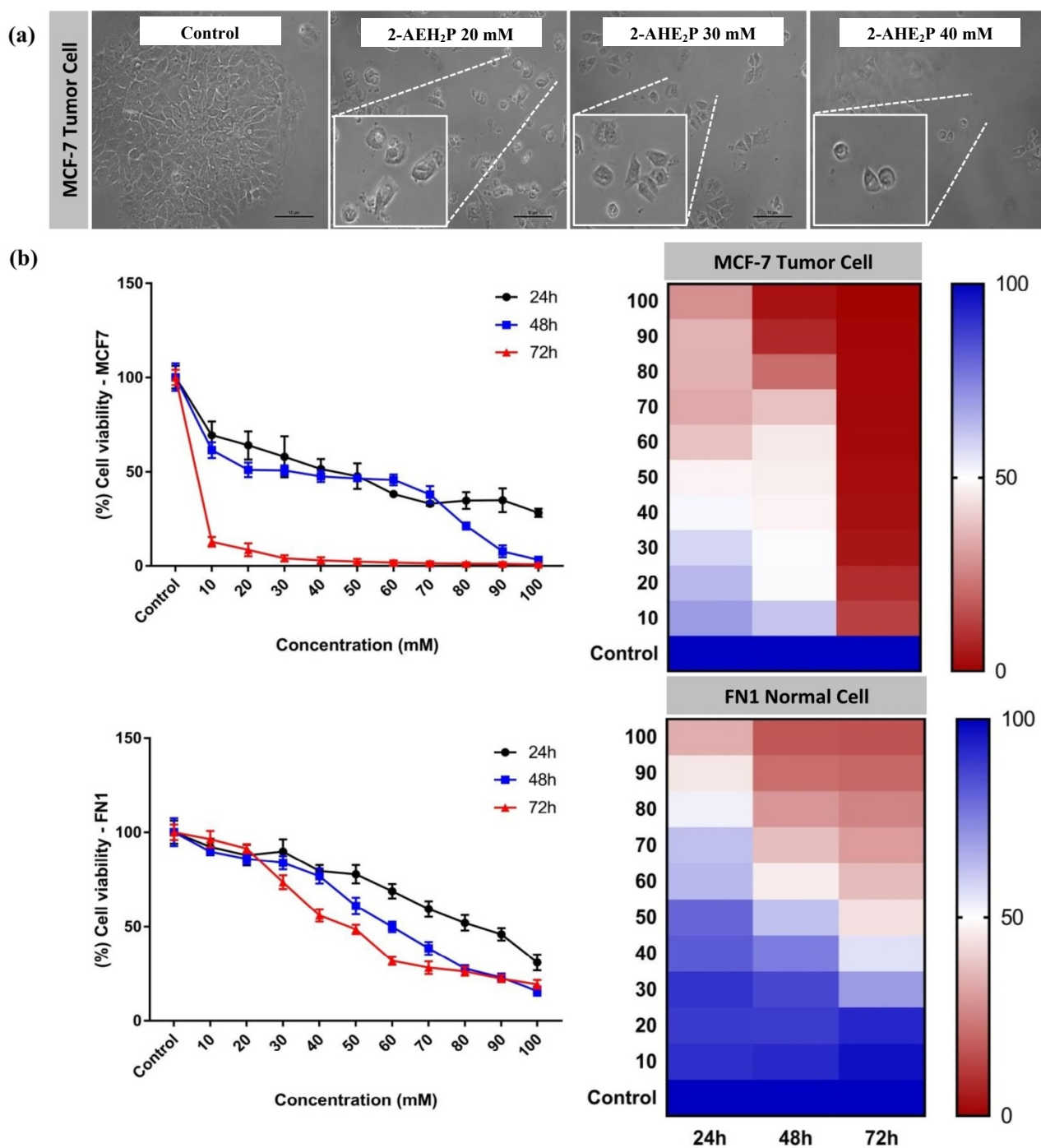


Fig. 1 Determination of cytotoxicity in MCF7 human breast tumor cells by the MTT colorimetric method. The cells were treated with different concentrations of monophosphester 2-AEH₂P in the period of 24, 48 and 72 h. (a) Photomicrographs of the morphological analysis of the tumor cells of the MCF7 treated in the 24 h period; (b) Heatmap shows the correlation of the cytotoxic effect expressed as mean \pm SD of three independent experiments.

Table 1 Table with IC_{50%} values for human breast cancer tumor cells MCF7 and normal human fibroblast FN1.

| Compounds | Cells | IC _{50%} Value (mM) | | |
|----------------------|-------|------------------------------|------|------|
| | | 24 h | 48 h | 72 h |
| 2-AEH ₂ P | MCF-7 | 37.2 | 25.8 | 1.8 |
| | FN1 | 81.8 | 51.6 | 44 |

These concentrations were chosen from the calculation of $IC_{50\%}$ obtained in different times. The percentage of MCF-7 tumor cells in the different phases of the cell cycle were quantified after treatments. Treatment 24 h with the 2-AEH₂P, the phases of the cell cycle change significantly compared to the control group. The G0/G1 cell cycle phase decreased significantly, while there is an arrest at the G2/M phase compared to the control group (Figure 2A).

In the treatment of 48 h with the 2-AEH₂P, the phases of the cell cycle change significantly compared to the control group. At the concentration of 20 mM, and the fragmented DNA G0/G1 phase increased significantly, while the phases S and G2/M decreased significantly (Figure 2B).

3.3 Confocal Laser Scanning

3.3.1 Rhodamine 123

MCF-7 tumor cells were photomicrographed in a laser confocal microscope, it is observed in the control group that photomicrograph marking of mitochondria was well defined and structured around the core. However, the groups treated with different concentrations of 2-AEH₂P, mitochondria are not intact and modify their distribution, preferably diffusion from the nucleus to the cytoplasm. It is noteworthy that the higher concentrations of 30 mM of 2-AEH₂P there is a significant reduction in cell density (Figure 3A).

3.3.2 Acridine-orange

After treatment with the 2-AEH₂P, at concentrations of 20 mM, there is the formation of lysosomal vacuoles distributed in the cytoplasm with morphological changes. In addition, there are changes in cellular structure, cell density decreased, as already mentioned in the previous results presented in this report (Figure 3B).

3.4 Measurement of Mitochondrial Membrane Potential

The analyzes on flow cytometer after labeling by fluorescent probe rhodamine 123 demonstrated that

treatment with 2-AEH₂P significantly decreased mitochondrial electrical potential compared to the control group, especially at a concentration of 40 mM 2-AEH₂P (Figure 3C).

3.5 Cellular Senescence

MCF-7 tumor cells were incubated with the 2-AEH₂P at concentrations of 10, 20, 30, 40 and 50 mM for 24 h of treatment. After, MCF-7 tumor cells have been subjected to enzymatic action of β -galactosidase. The cells were observed and the photos were taken using a light microscope and analyzed for the number of cells (10 fields) counted 100 cells/field (Figure 4A).

3.6 Proliferation Assay CFSE-DA

To characterize the proliferative activity of MCF-7 tumor cells treated with 2-AEH₂P and controls was carried out the proliferation assay with the marker carboxyfluorescein (CFSE-DA). MCF-7 tumor cells were treated with 2-AEH₂P at concentrations 20, 30 and 40 mM, for 24, 48 and 72 h. In all concentrations significant decrease in the proliferation rate (Figure 4B).

3.7 Evaluation of Apoptotic Activity with Annexin V/PI

MCF-7 tumor cells were treated with 2-AEH₂P for 24 h at concentrations of 20, 30 and 40 mM. At higher concentrations, a significant increase in the percentage of dead cells in late apoptosis and necrosis was observed. While in a lower concentration, showed a significant increase in late and early apoptosis, these data confirm the data obtained with the expression of Caspase active by flow cytometry (Figure 5).

3.8 Evaluation of Markers by Flow Cytometry

After treatment with 2-AEH₂P for 24 h, MCF-7 tumor cells were analyzed with control and of cell cycle progression markers (Caspase 3-8 active, Bax, Bad, Bcl-2, p53, TNF/R1, PCNA, Cytochrome C,

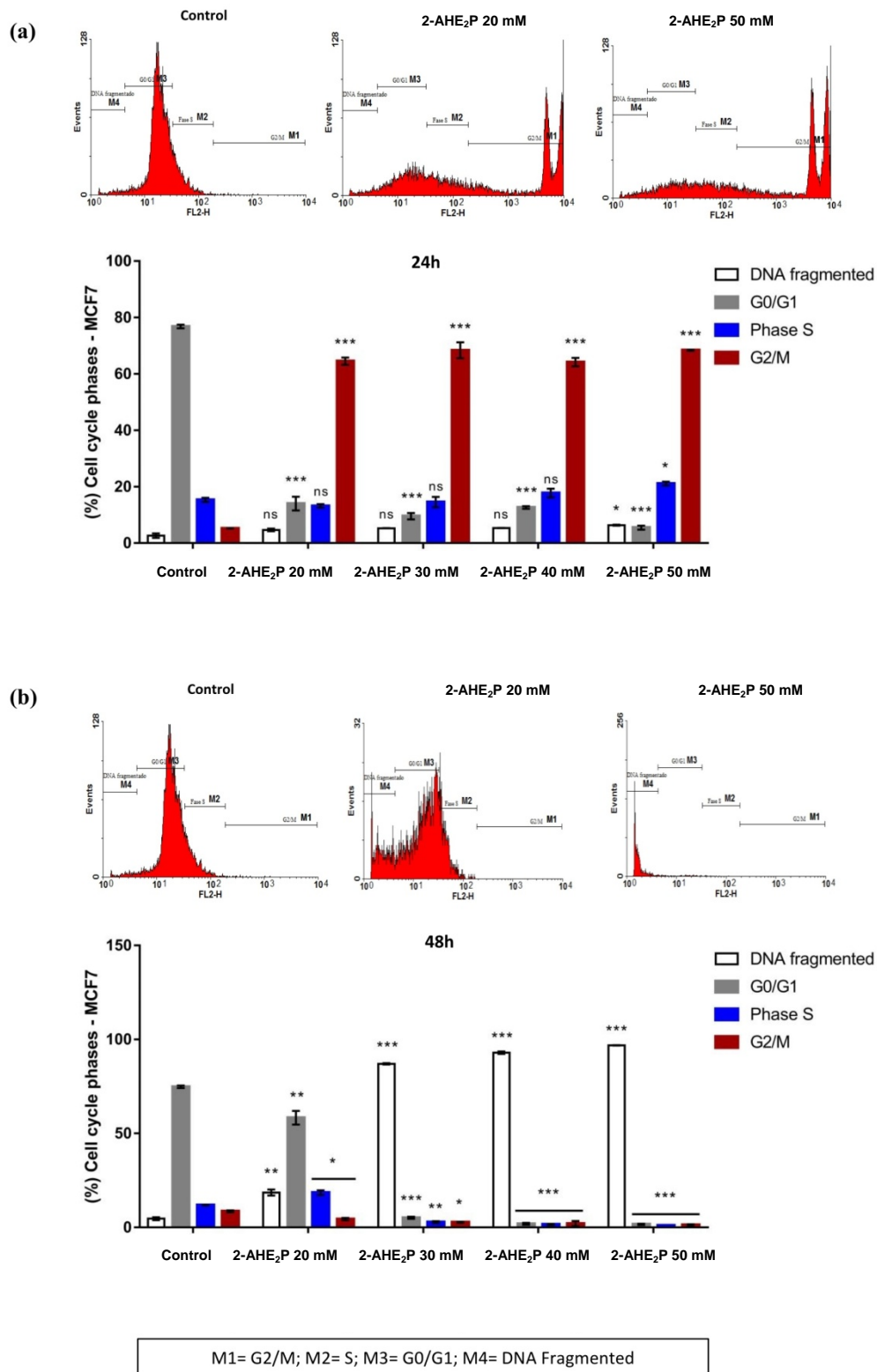


Fig. 2 Analysis of the cell cycle phases in MCF7 human breast cancer tumor cells. The cells were treated with the monophosphester 2-AEH₂P in the IC₅₀% values, for the period of 24 and 48 h. (a) Representative graphs of mean ± SD of cell cycle phases MCF7 tumor cells in control and treated with 2-AEH₂P for 24 h; (b) Representative graphs of mean ± SD of cell cycle phases MCF7 tumor cells in control and treated with 2-AEH₂P for 48 h. Significance values p* < 0.05 and p*** < 0.01, ANOVA obtained using variation of the test set for Tukey test. n = 3.

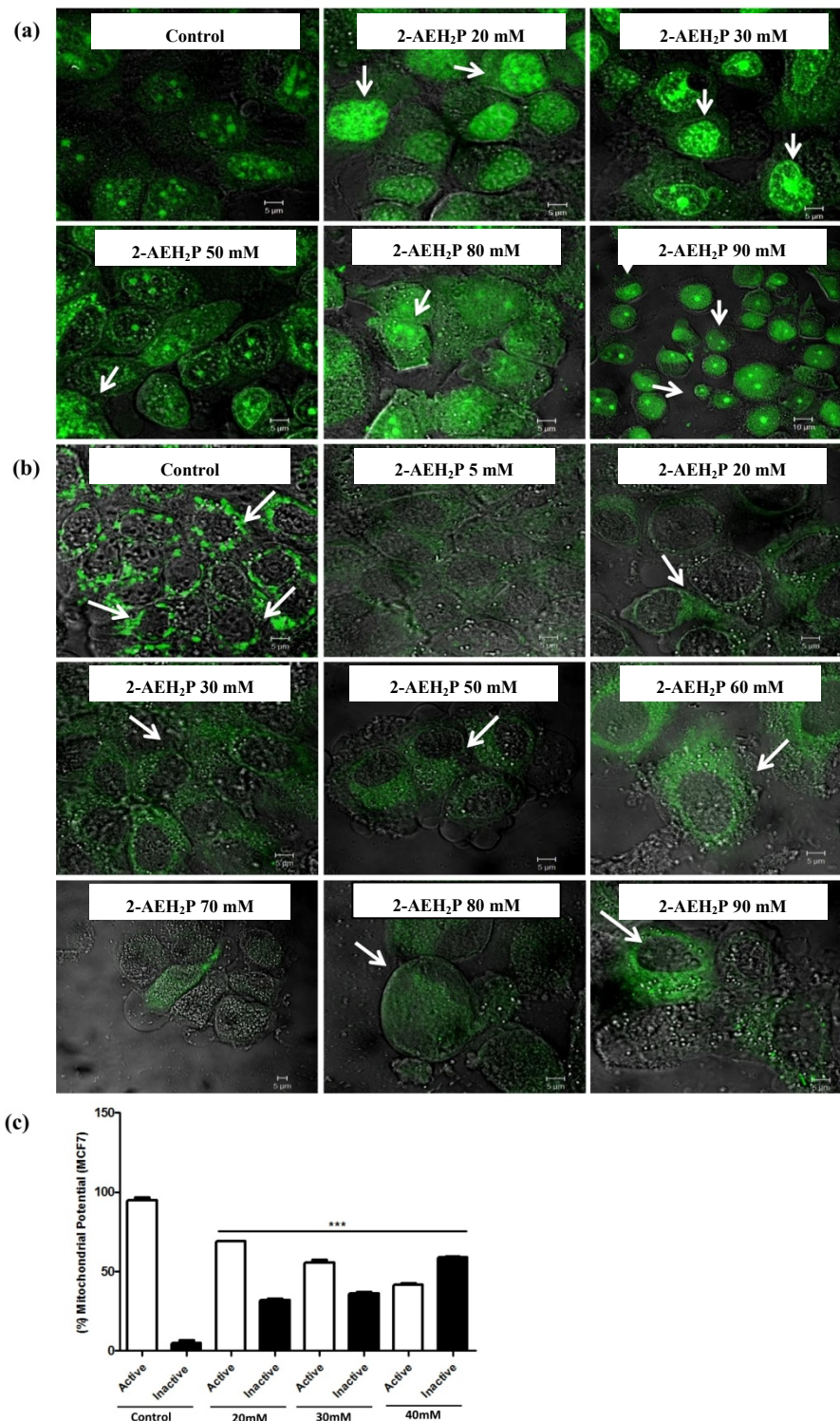


Fig. 3 Photomicrographs of MCF7 human breast cancer tumor cells marked with Rhodamine 123 and Acridine-orange, analyzed by laser confocal microscopy. Tumor cells treated with the 2-AEH₂P monophosphoester and at IC_{50%} values for a period of 24 h. (a) Photomicrograph of cellular aspects MCF7 tumor cells of the control groups and treated with different concentrations of Pho-s after 24 h and labeled with rhodamine 123; (b) Photomicrograph of cellular aspects MCF7 tumor cells of the control groups and treated with different concentrations of Pho-s after 24 h and labeled with acridine-orange; (c) Bar graph showing viable and non-viable mitochondria analyzed by flow cytometry. Significance values $p^* < 0.05$ and $p^{***} < 0.01$, ANOVA obtained by variation of the test followed using multiple test-Tukey Kremer. $n = 3$ experiments performed in triplicate.

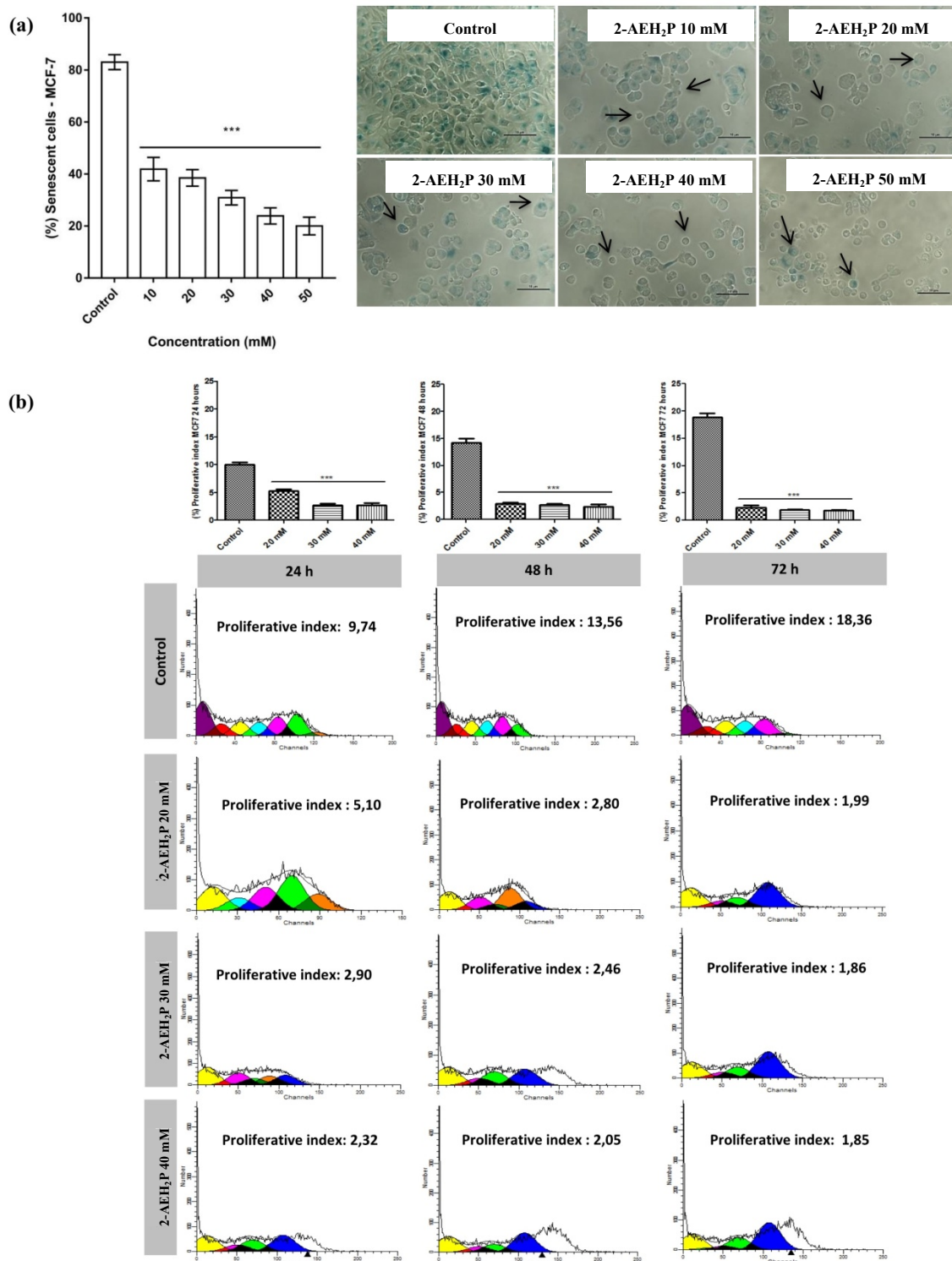


Fig. 4 Evaluation of proliferation and senescence of human breast tumor cells MCF7. The cells were treated with the monophosphate 2-AEH₂P in the IC₅₀ values, for the period of 24, 48 and 72 h. (a). Bar graphs of mean values \pm SD percentage of the population of MCF7 cells in senescence and photomicrograph of cellular aspects of the control and treated groups with the 2-AEH₂P and subjected to enzymatic activity of β -galactosidase; (b). Average values \pm SD bar graph of the proliferative MCF7 tumor cells treated with 2-AEH₂P 24 h and representative histograms in the flow cytometer proliferative index obtained using Wisard program Proliferation - WinMDI 2.9 Software. Significance values $p < 0.05$ and $p^{***} < 0.01$, ANOVA variation obtained using testing multiple test followed by Tukey-Kremer. Experiments $n = 3$, octuplicate.

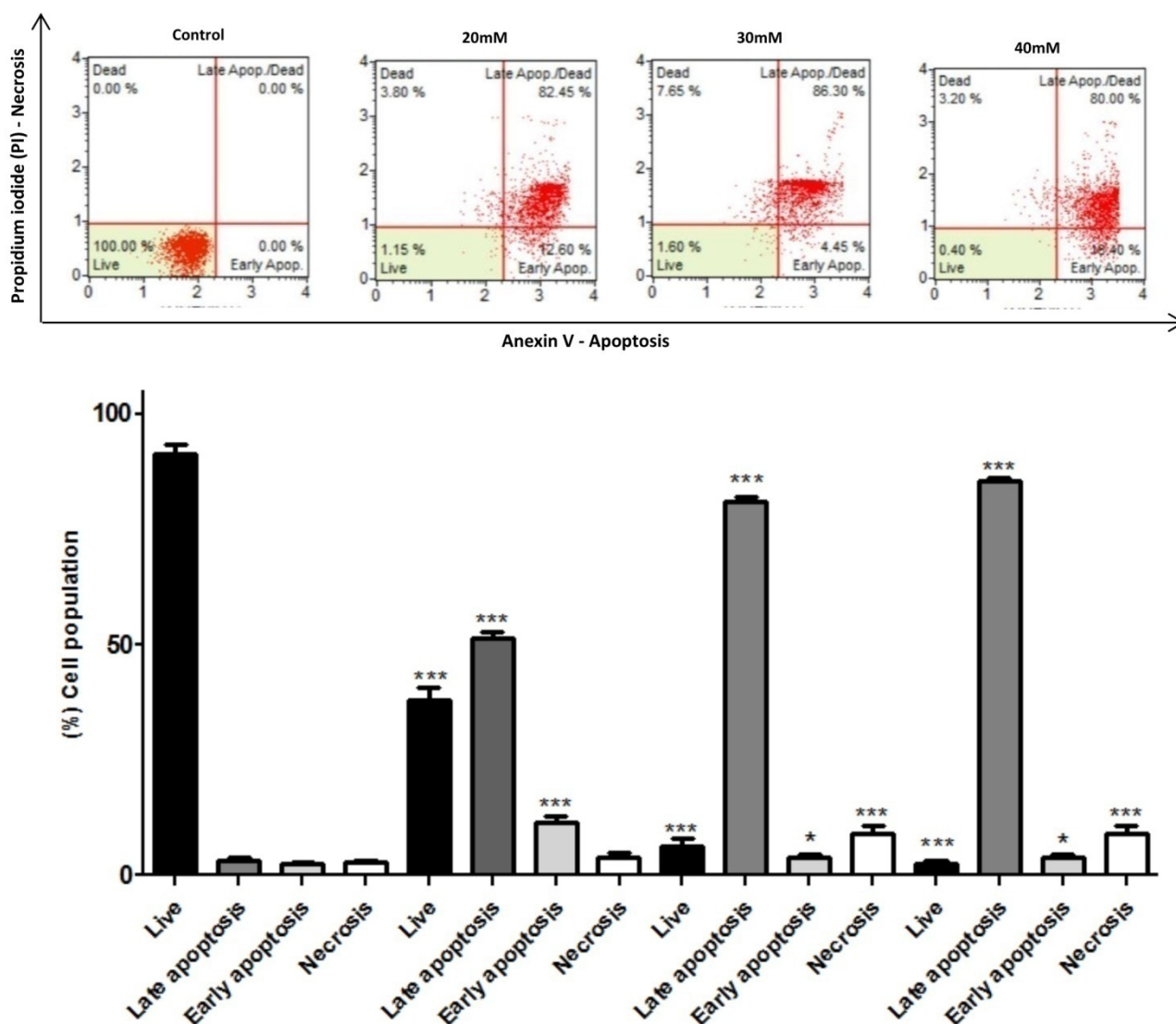


Fig. 5 Evaluation of cell death of human breast tumor cells MCF7. Bar graphs of mean values \pm SD percentage of the cell population of MCF7 cells treated with 2-AEH₂P at concentrations of 20, 30 and 40 mM. Dotplot representative of MCF7 cells distributed according to the type of cell death. Significance values $p^* < 0.05$ and $p^{***} < 0.01$, ANOVA obtained using variation of the test followed by multiple test-Tukey Kremer. $n = 3$ experiments performed in triplicate.

Cyclin D1). Data were acquired in flow cytometer (FACSCalibur) and analyzed by WinMDI version 2.9 software. Bcl-2 decreased significantly in the group treated with 2-AEH₂P, when compared to the control group. However, Bax and Bad increased significantly. Caspases actives 3 and 8 were increased in the group

treated with the 2-AEH₂P. TNF-R1 marker had an increased in the treated group.

Markers expression cyclin D1, p53 and cytochrome C had a significant increase in the group treated with the 2-AEH₂P, when compared to the control group (Figure 6).

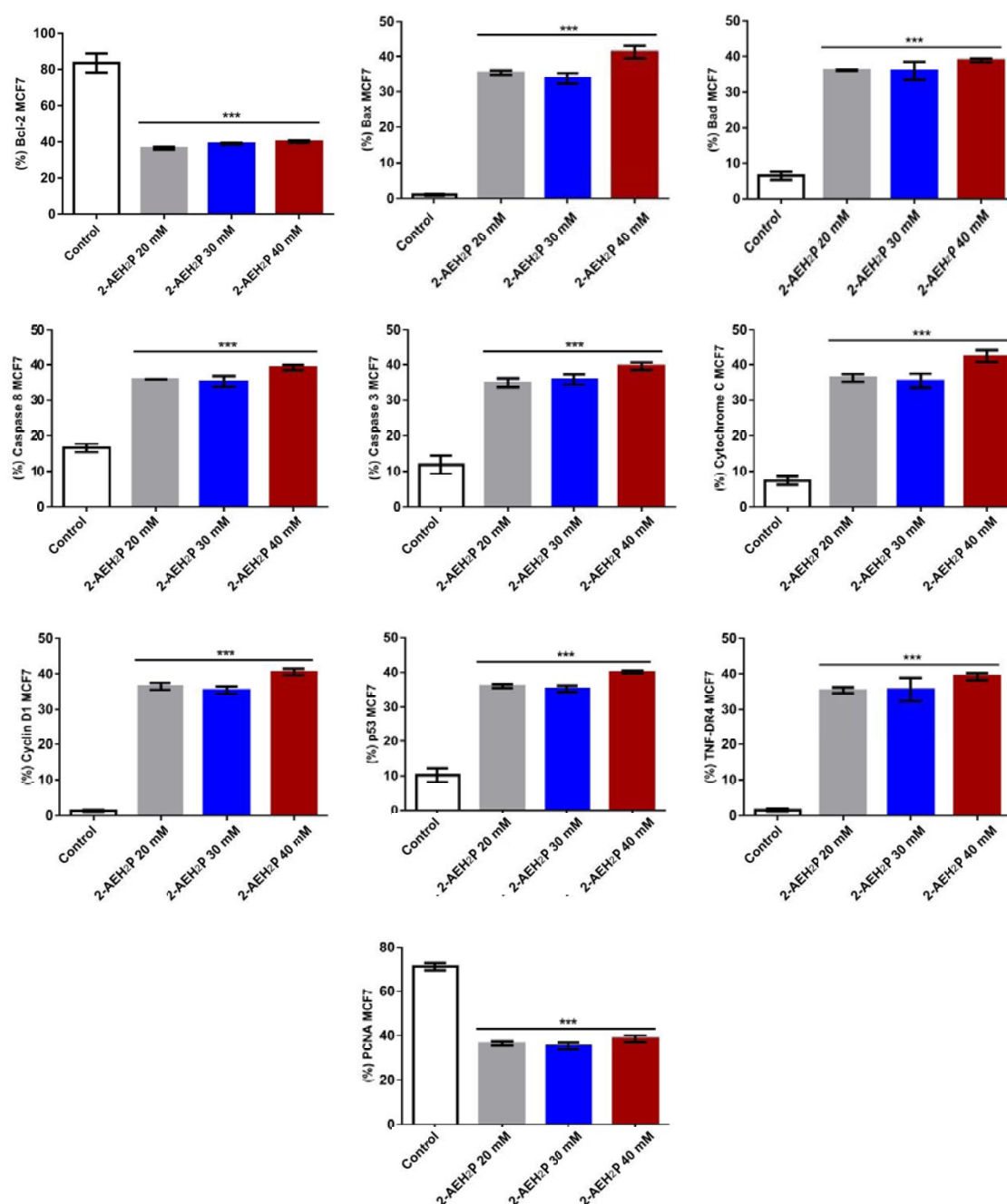


Fig. 6 Evaluation of the expression of proteins involved in cell death and proliferation. Average values of bar graphs \pm SD of percentage of expression of markers involved in apoptosis and cellular proliferation Bcl-2, Bax, Bad, Caspase 3, Caspase 8, Cytochrome C, Cyclin D1, p53 and TNF-DR4. Significance values $p^* < 0.05$ and $p^{***} < 0.01$, ANOVA obtained by variation of the test followed using multiple test-Tukey Kremer. $n = 3$.

4. Discussion

This study evaluated the potential cytotoxicity the monophosphate 2-AEH₂P in MCF-7 human breast adenocarcinoma cells. Several studies have

been published showing that, contrary to conventional chemotherapeutic agents, antineoplastic phospholipids act on tumor cell membranes, interfering with turnover of phospholipids. Due to its stability ether linkages which are not metabolised and can interfere

with signaling lipids, causing apoptosis in malignant tumor cells [21].

Corroborating data, the 2-AEH₂P was cytotoxic to all tumor cell lines studied by our research group, EAT (Ehrlich ascites tumor); B16F10 cells (murine melanoma); MCF-7 and MDA MB-231 cells (human breast cancer); H292 cells (lung cancer); SKMEL-28 and MEWO cells (human melanoma); K-562 and K-562 Lucena (Human Chronic Myeloid Leukemia) [14-20, 22-24]. However, treatment with the 2-AEH₂P was not cytotoxic to normal cells such as fibroblasts and endothelial cells [19, 20, 25]. The results of cytotoxicity tests indicate that the 2-AEH₂P promote their anti-tumor effects through a mechanism that appears to be common to all strains without promoting significant cytotoxic effects on normal cells [19].

Treatment with the 2-AEH₂P breast adenocarcinoma MCF-7 tumor cells proved to be effective in the ability to inhibit cell proliferation of different times. Cell viability was assessed after 24, 48 and 72 h of treatment with the 2-AEH₂P, leading to a reduction in cell viability. After 24 h MCF-7 breast adenocarcinoma cells showed aspects lysis and cell fragmented DNA formation. Data corroborate previous work of our group, in which treatment with 2-AEH₂P proved to be cytotoxic in MCF-7 cells [22]. However, after 48 and 72 h MCF-7 tumor cells showed increased cytotoxic effects at concentrations of 10 mM, with a percentage increase of cell death, loss of cell adhesion, fragmentation of the cytoplasmic membrane and loss of progression of cytoplasmic processes.

The analysis of cell cycle phases by flow cytometry revealed that MCF-7 tumor cells treated with different concentrations of 2-AEH₂P after 24 h showed that the proportion of stops cells in the G2/M phase increased with treatment, suggesting that 2-AEH₂P cell cycle arrest the effect of mitotic phase, these data corroborate Ferreira et al., who obtained a set of effects of 2-AEH₂P in murine melanoma cells B16F10 [14]. In the treatment with the 2-AEH₂P in time of 48

h, there was a significant increase in the percentage of cells that had fragmented DNA. This corroborates with the morphological changes observed after treatment; 2-AEH₂P was able to form cell aggregates, loss of adhesion and debris.

Senescence is the permanent stop of the growth occurring in response to any aging (senescence replication), or induced stress (premature senescence). Cellular senescence is directly related to the controls that occur in the cell during the cell cycle. In the G1 phase of the cycle, the cell undergoes internal and external monitoring aimed at ensuring the appropriate conditions for the division. To ensure that such intra and extracellular conditions are appropriate to correct replication of the genetic material in the S phase, there are two checkpoints in G1 [26]. MCF-7 tumor cells treated with the 2-AEH₂P and control were analyzed for enzymatic activity of β -galactosidase. There was a significant decrease in the number of senescent cells compared to the control group; this is because the treatment with the 2-AEH₂P significantly decreases the viability and cell number, data that corroborate the colorimetric MTT assay.

Tumor cells treated with the 2-AEH₂P were labeled with rhodamine 123 for visualization of mitochondria and its functionality by laser confocal microscopy. Tumor cells of the control group showed intracellular distribution, standard peri-nuclear mitochondria, whereas in treated group showed profound changes in mitochondrial morphology and mitochondria were presented dispersed in cytoplasm, not in the region around the nucleus.

Acridine orange is a nucleic-acid that binds to a cell, dying the living cells and emits green fluorescence when bound to dsDNA and red fluorescence when bound to ssDNA or RNA. This unique feature makes it useful for cell cycle studies. Acridine orange, has also been used as a lysosomal dying marker for cellular autophagy [27].

MCF-7 tumor cells treated with the 2-AEH₂P and control were subjected to staining with acridine-orange

and observed in a confocal laser microscope. Control group at a concentration of 5 mM of 2-AEH₂P presented a core marking and well-defined nucleoli. However, in the other treatment concentrations were observed marking and determination of heterochromatin. Whereas the 30 mM concentration of 2-AEH₂P, the cells underwent change in morphology, fragmentation of the cytoplasmic membrane and loss of cytoplasmic projections. At higher concentration, cells significantly lose cell adhesion.

Mitochondria are dynamic organelles which play a central role in the apoptotic process. The functional decrease in mitochondrial potential ($\Delta\Psi_m$) is known as a trigger for cell death by apoptosis, and this mechanism can be associated with the intrinsic apoptotic signaling pathway [28]. In a study of our group, with Ehrlich tumor cells, analysis of $\Delta\Psi_m$ showed that the effects of 2-AEH₂P are attributed to its ability to induce apoptosis by reducing the $\Delta\Psi_m$ [18]. These data corroborate the results obtained in this study; 2-AEH₂P induces the similar mechanism in MCF-7 tumor cells, indicating that the reduction of $\Delta\Psi_m$ may be the key event for triggering a cascade of signaling apoptosis.

In this study, the release of cytochrome c from the mitochondria correlates with the reduction of Bcl-2, indicating that 2-AEH₂P induced apoptosis in MCF-7 cells via the mitochondrial pathway. It is worth mentioning that MCF-7 cells are deficient in caspase-3 and an unexpected finding was that 2-AEH₂P induces the activation of caspase-3, detected by the cleavage of a specific substrate of caspase-3, Ac-YVAD-AMC [23, 29, 30]. Interestingly, he reveals that biochemical and morphological changes, typical of apoptosis, can be mediated by an activity similar to caspase-3 in MCF-7 tumor cells. Therefore, we hypothesized a possible mechanism for the apoptotic effects of 2-AEH₂P on MCF-7 tumor cells via the mitochondrial pathway.

From these data, an analysis with annexin V/PI on cells treated with 2-AEH₂P to determine the

percentage of cells in early apoptosis, late and necrosis was performed. The data showed that the 2-AEH₂P induces death by apoptosis, as there was a significant increase apoptosis late at all concentrations. However, at the highest concentration, there was an increase in cell death by necrosis; these findings collaborate with data obtained by our research group [22].

Tumor cells were treated with 2-AEH₂P at concentrations of 20, 30 and 40 mM, for 24, 48 and 72 h, in all treatments, significantly decreased index cell proliferation. These data corroborate the experiments above; the 2-AEH₂P is capable of inducing distinct mechanisms of cell death by apoptosis and inhibits cell proliferation capacity, increasing the proportion of cells in senescence.

Our group has obtained significant results in the treatment of 2-AEH₂P in various tumor and normal cell lines. As this study was obtained from the calculation of the IC_{50%} values at different times of treatment with the 2-AEH₂P, morphological changes after treatment and observed by light microscopy and confocal changes in cell cycle phases, in addition to results with the cell markers expression and cell proliferation assay suggest the use of 2-AEH₂P as an antitumor agent capable of inducing cell death.

5. Conclusions

The IC_{50%} inhibitory concentrations obtained for the monophosphate 2-AEH₂P showed significant cytotoxicity in the tumor line MCF-7 at 24, 48 and 72 h. Treatment with 2-AEH₂P had antiproliferative activity, decreased viability and adherence, and showed that 2-AEH₂P induces apoptosis, causes DNA fragmentation and decreased proliferative response in tumor cells, with no effect on normal cells. The values obtained with the proliferation rate determined by the CFSE-DA assay determined that the effect on the proliferative response of MCF-7 tumor cells when treated with 2-AEH₂P corroborates the results obtained by the MTT assay. These data reinforce the

potential use of 2-AEH₂P as an antineoplastic drug.

Acknowledgement

Fundação de Amparo a Pesquisa do Estado de São Paulo – FAPESP (Process number 2014/02344-1) and Conselho Nacional de Desenvolvimento Científico e Tecnológico – CNPq (Process number 305056/2019-0).

Conflict of Interest

The authors declare that there are no conflicts of interest.

References

- [1] Siegel, R. L., and Miller, K. D. 2020. "Cancer Statistics, 2020" *CA A Cancer Journal for Clinicians* 70 (3): 1-24.
- [2] Instituto Nacional de Câncer José Alencar Gomes da Silva, *Estimate/2020 – Cancer Incidence in Brazil*, no. 1. Rio de Janeiro, 2019.
- [3] Miecznikowski, J. C., Wang, D., Liu, S., Sucheston, L., and Gold, D. 2010. "Comparative survival analysis of breast cancer microarray studies identifies important prognostic genetic pathways" *BMC Cancer* 10 (1): 573.
- [4] Liu, F., Wang, L., Perna, F., and Nimer, S. D. 2016. "Beyond transcription factors: How oncogenic signalling reshapes the epigenetic landscape" *Nat Rev Cancer* 16 (6): 359-372.
- [5] Amin, M. B., et al. 2017. "The Eighth Edition AJCC Cancer Staging Manual: Continuing to build a bridge from a population-based to a more 'personalized' approach to cancer staging" *CA. Cancer J Clin.* 67 (2): 93-99.
- [6] Gandhi, N., and Das, G. 2019. "Metabolic Reprogramming in Breast Cancer and Its Therapeutic Implications" *Cells* 8 (2): 89.
- [7] Baumann, J., Sevinsky, C., and Conklin, D. S. 2013. "Lipid biology of breast cancer" *Biochim Biophys Acta* 1831 (10): 1509-1517.
- [8] Menendez, J. A. 2009. "Fine-tuning the lipogenic/lipolytic balance to optimize the metabolic requirements of cancer cell growth: molecular mechanisms and therapeutic perspectives." *Biochimica et Biophysica Acta* 1801 (3): 381-391.
- [9] Buller, C. L., et al. 2008. "A GSK-3/TSC2/mTOR pathway regulates glucose uptake and GLUT1 glucose transporter expression" *Am J Physiol Cell Physiol* 295 (3): C836-43.
- [10] Whiteman, E. L., Cho, H., and Birnbaum, M. J. 2002. "Role of Akt/protein kinase B in metabolism" *Trends Endocrinol Metab* 13 (10): 444-51.
- [11] Turner, O., Phoenix, J., and Wray, S. 1994. "Developmental and gestational changes of phosphoethanolamine and taurine in rat brain, striated and smooth muscle" *Experimental Physiology* 79 (5): 681-9.
- [12] Morse, D. L., et al. 2009. "Characterization of breast cancers and therapy response by MRS and quantitative gene expression profiling in the choline pathway" *NMR Biomed* 22 (1): 114-27. doi: 10.1002/nbm.1318.
- [13] Bierhanzl, V. M., Riesová, M., Taraba, L., Čabala, R., and Seydlová, G. 2015. "Analysis of phosphate and phosphate containing headgroups enzymatically cleaved from phospholipids of *Bacillus subtilis* by capillary electrophoresis" *Anal Bioanal. Chem* 407 (23): 7215-20.
- [14] Ferreira, A. K., et al. 2012. "Synthetic phosphoethanolamine a precursor of membrane phospholipids reduce tumor growth in mice bearing melanoma B16-F10 and in vitro induce apoptosis and arrest in G2/M phase" *Biomed Pharmacother* 66 (7): 541-8.
- [15] Ferreira, A. K., Meneguelo, R., Pereira, A., Filho, O. M. R., Chierice, G. O., and Maria, D. A. 2013. "Synthetic phosphoethanolamine induces cell cycle arrest and apoptosis in human breast cancer MCF-7 cells through the mitochondrial pathway" *Biomed Pharmacother* 67 (6): 481-7.
- [16] Ferreira, A. K., Santana-Lemos, B. A. A., Rego, E. M., Filho, O. M. R., Chierice, G. O., and Maria, D. A. 2013. "Synthetic phosphoethanolamine has in vitro and in vivo anti-leukemia effects" *Br J Cancer* 109 (11): 2819-28.
- [17] Ferreira, A. K., Meneguelo, R., Neto, S. C., Chierice, G. O., and Maria, D. A. 2011. "Synthetic phosphoethanolamine induces apoptosis through caspase-3 pathway by decreasing expression of Bax/Bad protein and changes cell cycle in melanoma" *J Cancer Sci Ther* 3 (3): 53-59.
- [18] Ferreira, A. K., Meneguelo, R., Pereira, A., Filho, O. M. R., Chierice, G. O., and Maria, D. A. 2012. "Anticancer effects of synthetic phosphoethanolamine on Ehrlich ascites tumor: An experimental study" *Anticancer Res* 32 (1): 95-104.
- [19] A. C. de Lima Luna, et al. 2016. "Potential antitumor activity of novel DODAC/PHO-S liposomes" *Int J Nanomedicine* 11: 1577-1591.
- [20] T. de O. Conceição, Laveli-Silva, M. G., and Maria, D. A. 2019. "Phosphomonoester Phosphoethanolamine Induces Apoptosis in Human Chronic Myeloid Leukemia Cells" *Journal of Pharmacy and Pharmacology* 7 (7): 434-450.
- [21] Wim J van Blitterswijk and Marcel Verheij, 2008. "Anticancer Alkylphospholipids: Mechanisms of Action,

Cellular Sensitivity and Resistance, and Clinical Prospects” *Curr Pharm Des* 14 (21): 2061-74.

- [22] Ferreira, A. K. 2013. “Alquil fosfatado sintético precursor dos fosfolípidios de membrana celular com potencial efeito antitumoral e apoptótico em modelos de tumores experimentais”
doi:10.11606/T.5.2013.tde-20052013-145336.
- [23] Ferreira, A. K., Meneguelo, R., Pereira, A., Filho, O. M. R., Chierice, G. O., and Maria, D. A. 2013. “Synthetic phosphoethanolamine induces cell cycle arrest and apoptosis in human breast cancer MCF-7 cells through the mitochondrial pathway” *Biomed Pharmacother* 67 (6): 481-7.
- [24] Ferreira, A. K., et al. 2013. “Anti-Angiogenic and Anti-Metastatic Activity of Synthetic Phosphoethanolamine” *PLoS One* 8 (3): e57937.
- [25] Laveli-Silva, M. G., Luciana Bastianelli Knop, and Durvanei Augusto Maria. 2019. “Meclizine Chloridrate and Methyl- β -Cyclodextrin Associated with Monophosphoester Synthetic Phosphoethanolamine Modulating Proliferative Potential in Triple-Negative Breast Cancer Cells” *Journal of Pharmacy and Pharmacology* 7 (7): 408-420.
- [26] Xu, X., et al. 2014. “Inactivation of AKT induces cellular senescence in uterine leiomyoma” *Endocrinology* 155 (4): 1510-9.
- [27] Tatevik, S., Allison, T., Richa, A., Eltyeb, A., and Kristin, W. 2014. “Detecting apoptosis in Drosophila tissues and cells” *Methods* 68 (1): 89-96.
- [28] Galluzzi, L., Kepp, O., and Kroemer, G. 2011. “Mitochondrial dynamics: A strategy for avoiding autophagy” *Curr Biol* 21 (12): R478-80.
- [29] Ja, R. U. 2009. “MCF-7 breast carcinoma cells do not express caspase-3” *Breast Cancer Res Treat* 117 (1): 219-21.
- [30] Benjamin, C. W., Hiebsch, R. R., and Jones, D. A. 1998. “Caspase Activation in MCF7 Cells Responding to Etoposide Treatment” *Mol Pharmacol* 53 (3): 446-50.